ELSEVIER

Biochimica et Biophysica Acta 1276 (1996) 140–146

BBA Biochimica et Biophysica Acta

The distances from tyrosine D to redox-active components on the donor side of Photosystem II determined by pulsed electron-electron double resonance

Hideyuki Hara [a], Asako Kawamori [a,*,1], Andrei V. Astashkin [b], Taka-aki Ono [b]

[a] *Faculty of Science, Kwansei Gakuin University, Uegahara 1-1-155, Nishinomiya 662, Japan*
[b] *The Institute of Physical and Chemical Research (RIKEN), Wako, Saitama 351-01, Japan*

Received 29 November 1995; revised 16 April 1996; accepted 17 April 1996

Abstract

A pulsed electron-electron double resonance (ELDOR) method was applied to measure the dipole interactions between paramagnetic species on the donor side of Photosystem II. The distance between the Mn cluster and the redox-active tyrosine residue Y_D was determined to be 27 ± 0.2 Å in the S_2 state of the oxygen-evolving Photosystem II. In Ca^{2+}-depleted preparations the same distance was obtained from the measurement of the modified multiline signal. The distance between Y_D and the paramagnetic species giving rise to the split S_3 signal was found to be 30 ± 0.2Å.

Keywords: Calcium ion-depleted Photosystem II; Manganese-cluster; Multiline signal; S_3 signal; Electron spin echo; Electron-electron double resonance

1. Introduction

Photosystem II is composed of several intrinsic and extrinsic polypeptides with unknown structures. Among them, the heterodimer of D1 and D2 proteins is believed to bind almost all electron-transfer components of PS II, the Mn-cluster in OEC, the tyrosine donors Y_Z and Y_D, the primary electron donor P680, pheophytin, and the primary (Q_A) and secondary (Q_B) electron acceptor quinones [1–4].

On the donor side of PS II, a photooxidized P680 is reduced by the electron donated from Y_Z. Y_Z^+ is, then, reduced by the electron from the Mn-cluster that is oxidized stepwise through five catalytic states S_0-S_4 and finally produces an oxygen molecule [5]. In the S_2 state, the well-known multiline EPR signal of the Mn cluster in OEC is observed at cryogenic temperatures [6]. It exhibits a g-factor of 1.96 and a total width of about 200 mT, with about 19 partially resolved lines due to the hyperfine interactions of the Mn nuclei [6–8].

Ca^{2+} is an indispensable cofactor of the oxygen evolution. The depletion of Ca^{2+} from PS II blocks the transition somewhere beyond the S_2 state and deactivates the oxygen evolution activity. The S_2 state in Ca-depleted PS II membranes is dark-stable and exhibits a so-called modified multiline signal due to the Mn cluster in OEC, with greater width, increased number of lines and reduced hyperfine splittings as compared with the multiline signal in the oxygen-evolving PS II [9,10].

When the Ca-depleted PS II in the S_2 state is further illuminated, another signal formally corresponding to the S_3 state is induced. This signal is located at $g \approx 2$ and has an overall width of about 20 mT, with two peaks separated by about 15 mT. The origin of the S_3 signal is not yet established; however, several models are described in literature [11,12].

To elucidate the location of the electron carriers in PS II, the EPR measurements of the magnetic relaxation times [13–18] and a selective hole burning method have been applied [19]. From these measurements, the separation

Abbreviations: PS II, Photosystem II; Y_D, a tyrosine electron donor in D2 subunit of PS II; Y_Z, a tyrosine electron donor in D1 subunit of PS II; Chl, chlorophyll; Cyt, cytochrome; OEC, oxygen-evolving complex; Mops, 4-morpholinopropanesulfonic acid; Mes, 2-morpholinoethanesulfonic acid; m.w., microwave; EPR, electron paramagnetic resonance; ESE, electron spin echo; ELDOR, electron-electron double resonance; CW, continuous wave.

* Corresponding author. Fax: +81 798 510914.
[1] On leave from the Institute of Chemical Kinetics and Combustion, Russian Academy of Sciences, 630090 Novosibirsk, Russia.

PII S0005-2728(96)00071-0

between Y_D^+ and the Mn cluster was estimated to be in the range of 28–43 Å [14], 24–28 Å [17] or 28–30 Å [19]. The distance between Y_D^+ and Y_Z^+ was estimated to be 29–30 Å using the '2 + 1' ESE method [20,21].

The '2 + 1' ESE technique used in [20,21] is a special case of general electron-electron double resonance methods. It employs a sequence of three m.w. pulses with the same carrier frequency and is applicable when the EPR transitions of the studied paramagnetic centers can be efficiently excited by the pulses used. This implies that the EPR spectra of the studied species have to be reasonably narrow (of the order of one-two mT) and overlapping. The Y_D^+ and Y_Z^+ pair studied in Ref. [20,21] presents an example of this kind.

In this work, the dipole interactions between the paramagnetic species in PS II are probed by a pulsed ELDOR (ESE ELDOR) method [22,23]. The pulse sequence employed is same as that in the '2 + 1' ESE method, but the m.w. pulses with two different carrier frequencies are used. It allows one to study interactions between the paramagnetic centers with different resonant frequencies. In particular, this method allows one to estimate the distances between Y_D^+ and other paramagnetic species in PS II.

2. Materials and methods

The oxygen-evolving PS II membranes (500 μM O_2/mg Chl per h) were isolated from market spinach by the BBY method [24] with modifications described in Ref. [25] and suspended in the buffer medium containing 200 mM sucrose, 20 mM NaCl and 20 mM Mops/NaOH (pH 6.8), with 50% vol. glycerol added. The membranes with 12 mg Chl/ml were stored at 77 K until use.

For Ca^{2+}-depletion, the membranes at a Chl concentration of 0.5 mg/ml were suspended in a buffer 400 mM sucrose, 20 mM NaCl, 10 mM citrate/NaOH (pH 3.0) at 0°C for 5 min. Then, 10% vol. of 400 mM sucrose, 20 mM NaCl and 500 mM Mops/NaOH (pH 7.5) were added to adjust the final pH at about 6.5 as described in Refs. [26,27]. The treated membranes (denoted as Ca-depleted PS II) were washed and resuspended in a final buffer of 400 mM sucrose, 20 mM NaCl and 20 mM Mes/NaOH at pH 6.5. All procedures were done in complete darkness or under dim green light to preserve the S_1 state.

The illumination of the PS II membranes was done by a 500 W tungsten-halogen lamp through an 8-cm thick water filter at 0°C.

A part of the Ca-depleted membranes was preilluminated for 1 min and dark-adapted for 30 min to form a dark-stable S_2 state. Then, 50 μM DCMU was added to these membranes to ensure a single electron-transfer event beyond the S_2 state. The membranes with DCMU were collected by a centrifugation at 35 000 × g for 20 min and resuspended in the same buffer. The concentrations of both

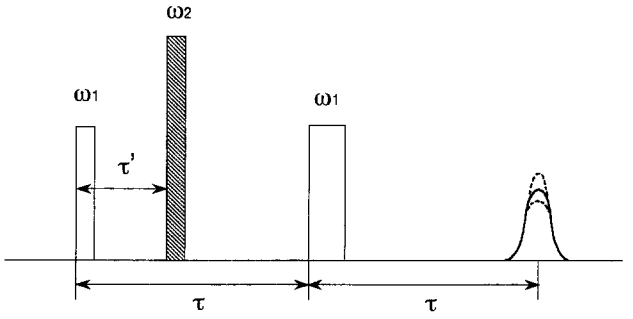

Fig. 1. The pulse sequence of the ESE ELDOR method. The primary ESE signal is formed by the first and third m.w. pulses with the carrier frequency ω_1, separated by the time interval τ. The amplitude of the ESE signal is observed as a function of the position τ' of the second m.w. pulse with the carrier frequency ω_2.

types of membranes (with and without DCMU) were about 20 mg Chl/ml.

The three types of membranes (oxygen-evolving PS II in the S_2 state, Ca-depleted PS II in the S_2 state with DCMU and in the S_1 state without DCMU) were transferred into Suprasil quartz tubes with the inner diameter of 4 mm and the height of 10 mm, and have been stored in liquid N_2 until the measurements.

The ESE ELDOR measurements have been performed on a pulsed EPR spectrometer ESP-380 (Bruker) using a pulse sequence shown in Fig. 1. The m.w. bridge of another CW EPR spectrometer ESP-300E (Bruker) was used as a second m.w. frequency source. The output of this bridge was fed into the resonator through the m.w. pulse former unit of the pulsed EPR spectrometer giving the second pulse in the pulse sequence shown in Fig. 1.

The pulsed EPR spectrometer was equipped with a cylindrical dielectric cavity (ER4117DHQ-H, Bruker), and a helium gas flow system (CF935, Oxford Instruments). The measurement temperature was about 6K and m.w. pulses of 16, 24 and 24 ns duration were used. The m.w. magnetic field amplitudes B_1 in these pulses were set to provide the spin rotation angles of 90°, 180° and 180°, respectively. The maximum attainable difference between the carrier frequencies of the first and third (ESE-forming) m.w. pulses and that of the second (pumping) m.w. pulse was about 150 MHz. This value is limited by the quality factor of the dielectric cavity ($Q \approx 100$ in our experiments). With this frequency difference we could excite an EPR spectrum in the regions separated by about 5 mT or by 150 MHz.

3. Theory

Consider a spin system composed of pairwise-distributed radicals, with every pair consisting of two types of spins, A and B. In the pulsed ELDOR method used in this work, the spin system is excited by three m.w. pulses (Fig. 1). The first and third pulses, separated by the time interval

τ, have a carrier frequency ω_1 resonant with the EPR transitions of spins A and form the primary ESE signal of these spins. The second pulse, separated from the first one by the time interval τ' ($\tau' \leq \tau$), has a carrier frequency ω_2. This pulse is resonant with spins B and changes their projections from $|\alpha\rangle$ to $|\beta\rangle$ and vice versa. If the magnetic dipole interaction between the pairwise-distributed spins is appreciable, the flip of the B spin changes the local magnetic field for its partner in the pair (A spin). As a result, the magnetization of the A spins after the third pulse cannot be completely refocused at the time 2 τ and the amplitude of the primary ESE signal exhibits an oscillating dependence on the second pulse position (i.e., on τ') [22,23]:

$$V(\tau,\tau') \propto 1 - p[1 - \cos(2\pi D\tau')] \quad (1)$$

where

$$D = D_o(1 - 3\cos^2\theta) \quad (2)$$

is the secular component of the dipole interaction between spins A and B. The value p ($0 \leq p \leq 1$) is a fraction of spins excited by the pumping pulse. It depends on the EPR spectrum width of spins B and on the pumping pulse intensity and duration [22,23].

From Eq. 1 it follows that the frequency of the oscillations in the dependence of the primary ESE signal on τ' (briefly, ELDOR trace) is determined by the dipole interaction and their amplitude is determined by the excitation factor p. The typical values $p \approx 0.3$ found in our experiments described below indicate an incomplete excitation of the Y_D^+ signal by the pumping pulse. This result is not surprising as the Y_D^+ spectrum width (≈ 2 mT) is larger than the excitation width of the 180° pumping pulse of 24 ns duration (≤ 1.4 mT). Besides, the non-oscillating background due to Cyt b559 also contributes to all ELDOR traces recorded in this work (see below), thus decreasing the effective p-values. As the p-values are of no special importance in this study, they will not be discussed further.

In a nonoriented system Eq. 1 is to be averaged over the angle θ between the radius-vector $\mathbf{r}$ connecting the radicals in pair, and the direction of the external magnetic field $\mathbf{B_o}$:

$$\langle V(\tau,\tau')\rangle \propto \int_o^{\pi} V(\tau,\tau')\sin\theta d\theta \quad (3)$$

From the value of the dipole interaction D_o determined in the ELDOR experiment, the distance between the radicals can be found using a point-dipole approximation:

$$D_o = (g\beta)^2/hr^3 \quad (4)$$

4. Results and discussion

4.1. Oxygen-evolving PS II

Let us consider the results obtained for the oxygen-evolving PS II. The field-sweep primary ESE spectrum

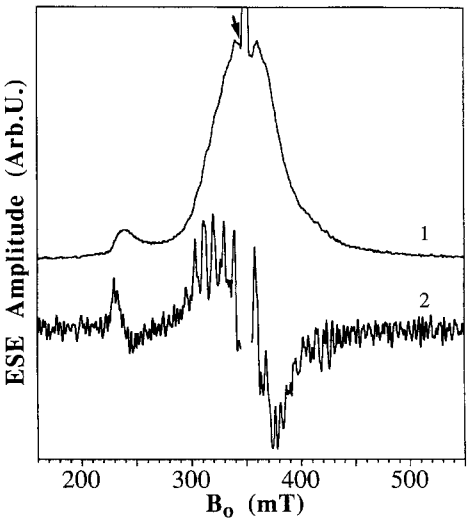

Fig. 2. Trace 1, primary ESE field sweep at $\tau = 200$ ns observed in the oxygen-evolving PS II in the S_2 state after illumination for 5 min at 230 K Trace 2, numerical first derivative of trace 1. The arrowhead shows the magnetic field satisfying the condition $\omega_1 = g\beta B_0$ in the ELDOR experiment (see Fig. 3). The measurement conditions: temperature, 6 K; pulse repetition time, 1 ms.

measured in the S_2 state at the temperature of 6 K is shown by trace 1 in Fig. 2. The narrow over scaled peak in the center of this spectrum is due to Y_D^+. The broad signal is contributed by Cyt b559 and Mn cluster in the S_2 state. The presence of the cytochrome signal is evident from the characteristic shoulder at $g \approx 3$. The contribution of the Mn multiline signal is best demonstrated by trace 2 showing a first derivative of trace 1.

The ESE ELDOR experiment was performed at a fixed $\tau = 1000$ ns, with τ' varying from 8 to 960 ns. The external magnetic field B_0 was 345 mT. The m.w. frequency of the pumping pulse $\omega_2/2\pi \approx 9.68$ GHz at this magnetic field resonated with Y_D^+ signal ($g \approx 2.0046$). The m.w. frequency of the first and third pulses $\omega_1/2\pi \approx 9.79$ GHz resonated with the Mn multiline signal, as shown by an arrow in Fig. 2. The 0.11 GHz difference between ω_1 and ω_2 corresponds to the difference in the resonant magnetic fields of about 4 mT.

The ELDOR trace recorded for the oxygen-evolving PS II in the S_2 state is shown in Fig. 3 by open squares. The oscillations observed in this trace are due to the dipole interaction between Y_D^+ and some of the paramagnetic centers contributing to the ESE signal, i.e., Mn cluster in OEC or Cyt b559, or both of them. If the carrier frequency of the pumping pulse was out of resonance with Y_D^+, no oscillations were observed.

To decide, which of these centers gives the oscillations in the ELDOR trace in Fig. 3, we have repeated the experiment at the temperature of 12 K. At this temperature the Mn multiline ESE signal decayed with a time constant T_2 (spin-spin relaxation time), before observation at 1000 ns. Then the ESE signal is contributed only by Cyt b559.

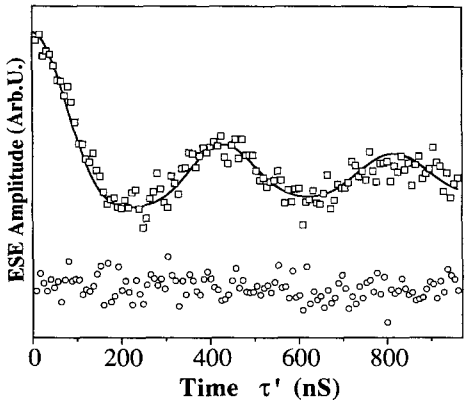

Fig. 3. Open circles and squares, the dependences of the primary ESE signal of the oxygen-evolving PS II in the S_1 and S_2 states on τ', respectively. The solid line is calculated using Eq. (3) for the dipole interaction constant $D_0 = 2.6$ MHz. Experimental conditions: temperature, 6 K; pulse repetition time 1 ms; $\omega_1/2\pi \approx 9.79$ GHz; $\omega_2/2\pi \approx 9.68$ GHz; $\tau = 1000$ ns; $B_0 = 345$ mT.

In this experiment, however, no oscillations were observed. The ELDOR trace of the PS II sample in the S_1 state (open circles in Fig. 3) also did not show any clear oscillations. This result implies that the distance from Y_D^+ to the hem iron of Cyt b559 is fairly large, probably, greater than 47 Å calculated from Eq. 4, as the oscillation frequency should be smaller than 0.5 MHz $\leq 1/2\tau$. This result is consistent with the previous experiments to prove no effect of Cyt b559 on the spin-lattice relaxation rate of Y_D^+ [17,18]

Thus, the oscillations in Fig. 3 are caused by the dipole interaction of Y_D^+ with the Mn cluster in OEC. To determine the value of this interaction, the calculations were done using Eq. 3. As a result of these calculations, the value $D_0 = 2.6 \pm 0.03$ MHz was found. From D_0, using Eq. 4, one can estimate $r = 27.1 \pm 0.15$ Å. This value is consistent with the distance between Y_D^+ and the Mn cluster in PS II derived previously by a selective hole-burning method [19], indicating that the latter method, though not as direct as ELDOR, also gives a reliable information on the distances between paramagnetic centers.

4.2. Ca-depleted PS II

Trace 4 in Fig. 4 shows a field-sweep ESE spectrum of Ca-depleted PS II in the S_1 state. The same as in Fig. 2, the central part of this spectrum shows an intense narrow signal due to Y_D^+. The broad signal of lower intensity is due to Cyt b559.

After illumination of this sample for one minute and dark-adaptation for one hour at 0°C the Ca-depleted PS II was converted into the S_2 state exhibiting a modified Mn-multiline signal (trace 1 in Fig. 4). Trace 5 in Fig. 4 shows a first derivative of trace 1. The hyperfine structure visible in trace 5 confirms the formation of the modified Mn multiline signal.

After illumination of this sample for 5 s at 0°C the amplitude of the modified Mn multiline signal decreased and a signal with a doublet splitting of about 15 mT appeared around the center of the spectrum (Fig. 4, trace 2). The same signal was generated by illumination of a Ca-depleted PS II with DCMU added in the S_2 state (Fig. 4, trace 3). As only one electron transfer event is possible in the presence of DCMU, this signal is attributed to an S_3 state.

The amplitude of the S_3 signal in the sample with DCMU was about 30% smaller than that in the sample without DCMU. Therefore, to obtain better signal-to-noise ratio in the ESE ELDOR measurement of the dipole interaction between Y_D^+ and the species giving rise to the S_3 signal, the sample without DCMU was used.

The ELDOR measurement of the Ca-depleted PS II sample in the S_1 state, same as that for the oxygen-evolving PS II in the S_1 state has shown no oscillations due to the dipole interaction between Y_D^+ and Cyt b559 (data not shown). Thus, the cytochrome does not contribute to the oscillations in the ELDOR traces presented below.

The open squares in Fig. 5a show an ELDOR trace obtained for the Ca-depleted PS II sample in the S_2 state. The experimental settings were same as those in similar measurement of oxygen-evolving PS II. The ESE signal observed was due to the Mn multiline and Cyt b559, and

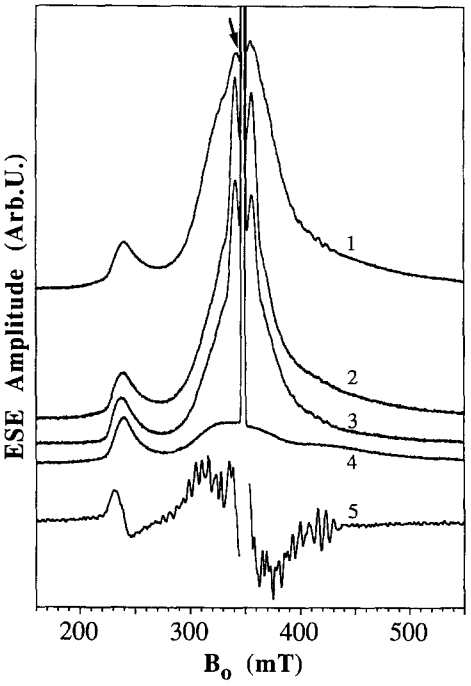

Fig. 4. Primary ESE field sweeps at $\tau = 200$ ns recorded in the Ca-depleted PS II. Traces 4, 1 and 2 are recorded in the sample without DCMU in the S_1, S_2 and S_3 states, respectively. Trace 3, the sample with DCMU added in the S_2 state, illuminated for 1 min at 0°C to generate the S_3 state. Trace 5, numerical first derivative of trace 1. The arrowhead shows the magnetic field satisfying the condition of $\omega_1 = g\beta B_0$ in the ELDOR experiment (see Fig. 5). The measurement conditions are same as in Fig. 2.

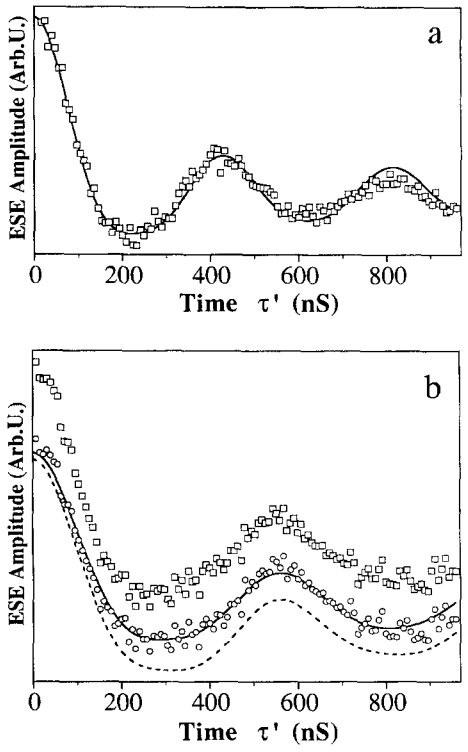

Fig. 5. (a) Open squares, the dependence of the primary ESE signal of the Ca-depleted PS II without DCMU in the S_2 state on τ' at $B_o = 345$ mT. The solid line is calculated using Eq. (3) for the dipole interaction constant $D_o = 2.6$ MHz. (b) Open squares, the dependence of the primary ESE signal of the Ca-depleted PS II without DCMU in the S_3 state on τ' at $B_o = 345$ mT. Open circles, same dependence after subtraction of the 15% contribution due to the modified Mn multiline (Fig. 5a, open squares). The solid line is calculated using Eq. (3) for the dipole interaction constant $D_o = 1.99$ MHz. The broken line is calculated using Eq. (6) for the dipole interaction constant $D_o = 1.99$ MHz and the angle $\theta' = 70°$ (see text). The experimental conditions are same as in Fig. 3.

the pumping pulse excited the spectrum of Y_D^+. Thus, the oscillations in the ELDOR trace are due to the dipole interaction between the Mn cluster and Y_D^+. The dipole interaction ($D_o \approx 2.6$ MHz) and the distance between these species ($r \approx 27$ Å) in Ca-depleted PS II are the same as those found above for the oxygen-evolving PS II (see the simulated solid trace in Fig. 5a).

The open squares in Fig. 5b show the ELDOR trace obtained for the Ca-depleted PS II in the S_3 state. The low-frequency oscillations in this trace are contributed by the S_3 signal and by the non-converted Mn multiline. The contribution of the Mn multiline signal was estimated to be about 15% from the field-sweep ESE spectra recorded at $\tau = 1000$ ns, i.e., same as for the ELDOR experiment (see Fig. 6). This contribution should be smaller than that in CW EPR signal detection, because the T_2 value for the multiline ESE is smaller than for the S_3 signal. The ratio of S_3 to S_2 state is not important for our purpose to detect dipolar interaction between the S_3 signal species and Y_D^+. We found that the S_3 and multiline signals could be assigned to different PS II centers and the ELDOR oscillation was of additive character.

The open circles in Fig. 5b show the ELDOR trace obtained from the experimental one (open squares) after subtraction of 15% of the ELDOR trace for Mn multiline (Fig. 5a). One can see, however, that only minor changes were introduced with this correction and the oscillation frequency in both traces is considerably lower than that observed for Mn multiline.

The calculation using Eq. 3 allows one to determine the dipole interaction $D_o = 1.99 \pm 0.03$ MHz that corresponds to the distance $r = 29.7 \pm 0.15$ Å. The ELDOR trace simulated with these parameters is shown by a solid line in Fig. 5b.

The S_3 signal shape is explained in literature as originating from dipole and exchange interactions between two paramagnetic centers [11,12] that we will denote R_1 and R_2. The origin of these species is not important for the interpretation of the results of the ELDOR experiment. However, the following consideration has to be taken into account. The m.w. pulses in our experiment excite only a small fraction of spins contributing to the S_3 signal. If the dipole term in the interaction of R_1 and R_2 prevails, the excited spins correspond to only a limited set of orientations of the radical pair R_1R_2 and, consequently, to a limited set of the orientations of PS II membranes. The calculation based on the contribution of all orientations (see Eq. 3) then becomes formally invalid.

Let us consider a limiting situation of the shape of the S_3 signal determined by the electron-electron dipole interaction only:

$$D_{12} = D_{12o}\left(1 - 3\cos^2\theta_{12}\right) \quad (5)$$

where θ_{12} is the angle between the static magnetic field B_o and the radius-vector r_{12} joining R_1 and R_2. The splitting between the peaks of the S_3 signal is about 15 mT and the m.w. pulses excite the spectrum region shifted

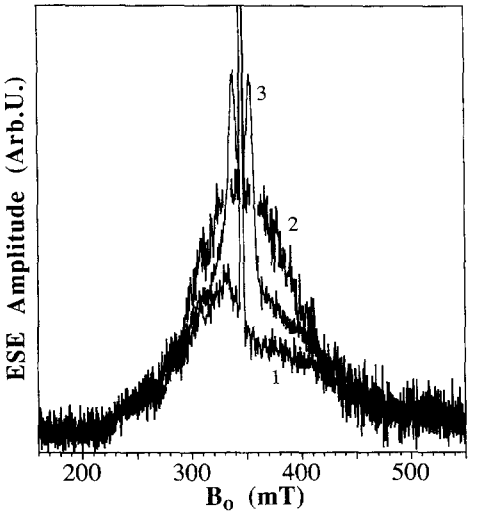

Fig. 6. Traces 1, 2 and 3 are the primary ESE field sweeps at $\tau = 1000$ ns recorded in the Ca-depleted PS II without DCMU in the S_1, S_2 and S_3 states, respectively. The measurement conditions are same as in Fig. 2.

about 4 mT from the center of this spectrum. Using Eq. 5, we can estimate the angles θ_{12} to be about 67° and 44°. However, a considerable width of the S_3 signal peaks ($\Delta B_{wd} \approx 8$ mT) leads to a noticeable contribution of other orientations to the ESE signal with a weighting factor

$$P \propto \exp\left[-(2)^{3/2}\Delta B^2/\Delta B_{wd}^2\right] \quad (6)$$

where ΔB is a magnetic field difference between the resonance field (for the angles θ_{12} of 67° and 44°) and the field corresponding to any other orientation.

To calculate the ELDOR effect for any given orientation of the radius-vector $\mathbf{r}_{12}$, we have to set in Eq. 2 $\cos\theta = \cos\theta_{12}\cos\theta' - \sin\theta_{12}\sin\theta'\cos\varphi$ and use the following expression instead Eq. 3:

$$\langle V(\tau,\tau')\rangle \propto \int_0^{\pi} V(\tau,\tau')\,d\varphi \quad (7)$$

Here the angle φ refers to the rotation around $\mathbf{r}_{12}$ and θ' is the angle between $\mathbf{r}_{12}$ and the radius-vector $\mathbf{r}$ joining the radical pair R_1R_2 with Y_D^+. We do not specify the origin of $\mathbf{r}$ because the distance $r_{12} \approx 5$–6 Å (as found from the splitting between the maxima of the S_3 signal) is much smaller than the distance from the radical pair to Y_D^+.

The calculation using Eqs. 1, 2, 5 and 6 allows one to fit the experimental ELDOR trace in Fig. 5b with $D_0 \approx 1.99 \pm 0.03$ MHz ($r \approx 29.7 \pm 0.15$ Å) and $\theta' \approx 70° \pm 10°$. One can see that the estimate of the dipole interaction value coincides with that obtained using Eq. 3. This is not surprising because at θ' close to 90° the full possible range of the orientations (0°–90°) of the radius-vector $\mathbf{r}$ with respect to the static magnetic field $\mathbf{B}_0$ is realized.

The value of θ' close to 90° allows one with a good accuracy to associate the value $r \approx 30$ Å with the distance from Y_D^+ to the center of the radius-vector $\mathbf{r}_{12}$ or with the distance from Y_D^+ to one of the species (R_1 or R_2) responsible for the S_3 signal.

Thus, using the ESE ELDOR method in this work we have determined the distances from Y_D^+ to the Mn cluster in OEC (about 27 Å) and to the species responsible for the formation of the S_3 signal in Ca-depleted PS II (about 30 Å). The difference between these distances is considerably larger than the experimental error of the order of 0.15 Å. Taking into account a typical size of the paramagnetic centers involved of the order of several Å, one has to interpret these distances as those between the centers of gravity of corresponding spin density distributions.

The distance between Y_D^+ and the species giving rise to the S_3 signal in Ca-depleted PS II (R_1 or R_2, see above) is similar to that between Y_D^+ and Y_Z^+ determined previously using a '2 + 1' ESE method [20,22]. It is tempting therefore to associate this species with Y_Z^+, which we denote R_1. This assignment would agree with the suggestion put forward recently by Gilchrist et al. [12] who found the ENDOR spectra of the S_3 signal and Y_Z^+ to be similar. The second paramagnetic center (R_2) was postulated to be the Mn cluster in OEC [12]. Such assignment of R_2 does not contradict the results of this work because, as already noted above, the distance derived from the ELDOR experiment is insensitive to the spin state of the paramagnetic centers. However, the assignment of R_2 to the Mn cluster is in conflict with the results of the measurements of the magnetic relaxation enhancement of Y_Z^+ in the S_1 state of Ca-depleted PS II that show the distance between Y_Z^+ and the Mn cluster to be 15–20 Å [21]. Our recent data also show that the dependence of the two-pulse ESE of the S_3 signal on the m.w. magnetic field B_1 cannot be explained by the assumption R_2 to be the Mn cluster in OEC. The latter will be published elsewhere. Thus we consider the origin of the S_3 signal, at least the species R_2, to be not yet completely established.

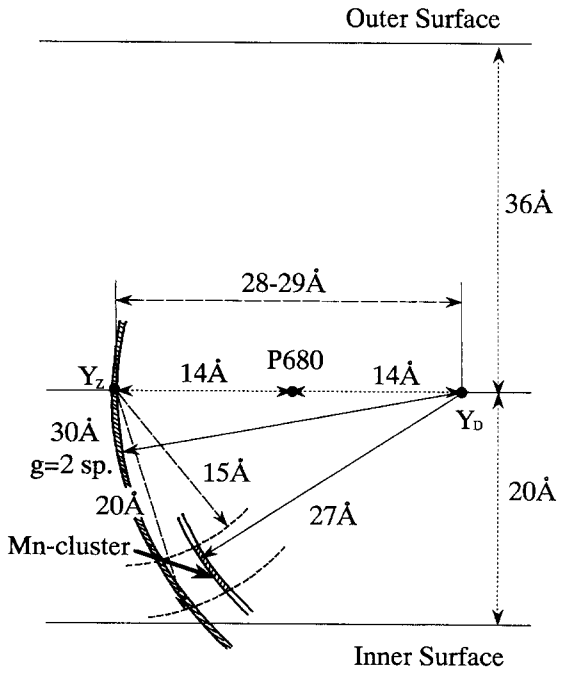

Fig. 7. Summary of the distances between paramagnetic species on the donor side of Ca-depleted PS II. The distance between Y_D and Y_Z has been recalculated from [21]. The position of P680 is assumed to be in the middle of the distance between Y_D and Y_Z. The distances of Y_D and Y_Z from the membrane surfaces are assumed to be same. The distance between Y_Z and the Mn cluster has been obtained by the measurement of the longitudinal relaxation time T_1 of Y_Z^+ in the S_1 state [21]. The sizes of each area show error ranges of the center of gravity of spin distributions.

The information on the distances between the redox-active species on the donor side of PS II obtained in this work and in Ref. [21] is collected in Fig. 7.

Acknowledgements

This work was supported by Grants-in-Aid for General Research (06452073) from Ministry of Education, Science and Culture of Japan. The authors thank Prof. Yu.D. Tsvetkov for useful advice about the pulsed ELDOR.

A.V.A. is grateful to Dr. H. Hayashi, the head of the Molecular Photochemistry laboratory at RIKEN, for hospitality and financial support.

References

[1] Debus, R.J., Barry, B.A., Babcock, G.T. and McIntosh, L. (1988) Proc. Natl. Acad. Sci. USA 85, 427–430.
[2] Vermaas, W.F.J., Rutherford, A.W. and Hansson, O. (1988) Proc. Natl. Acad. Sci. USA 85, 8477–8481.
[3] Svensson, B., Vass, I., Cedergren, E. and Styring, S. (1990) EMBO J. 7, 2051–2059.
[4] Ruffle, S.V., Donnelly, D., Blundell, T.L. and Nungent, J.H.A. (1992) Photosyn. Res. 34, 287–300.
[5] Kok, B., Forbush, B. and McGloin, M. (1970) Photochem. Photobiol. 11, 457–475.
[6] Dismukes, G.C. and Siderer, Y. (1981) Proc. Natl. Acad. Sci. USA 78, 274–278.
[7] Debus, R.J. (1992) Biochim. Biophys. Acta 1102, 269–352.
[8] Miller, A.-F. and Brudvig, G.W. (1991) Biochim. Biophys. Acta 1056, 1–18.
[9] Ono, T. and Inoue, Y. (1990) Biochim. Biophys. Acta 1015, 373–377.
[10] Boussac, A. and Rutherford, A.W. (1988) Biochemistry 27, 3476–3483.
[11] Boussac, A., Zimmermann, J.-L., Rutherford, A. W. and Lavergne, J. (1990) Nature 347, 303–306.
[12] Gilchrist, M.L., Jr., Ball, J.A. Rndall, D.W. and Britt, R.D. (1995) Proc. Natl. Acad. Sci. USA in press.
[13] Styring, S.A. and Rutherford, A.W. (1988) Biochemistry 27, 4915–4923.
[14] Evelo, R.G., Styring, S., Rutherford, A.W. and Hoff, A.J. (1989) Biochim. Biophys. Acta 973, 428–442.
[15] Innes, J.B. and Brudvig, G.W. (1989) Biochemistry 28, 1116–1125.
[16] Isogai, Y., Itoh, S. and Nishimura, M. (1990) Biochim. Biophys. Acta 1017, 204–208.
[17] Kodera, Y., Takura, K. and Kawamori, A. (1992) Biochim. Biophys. Acta 1101, 23–32.
[18] Hirsh, D.J., Beck, W.F., Innes, J.B. and Brudvig, G.W. (1992) Biochemistry 31, 532–541.
[19] Kodera, Y., Dzuba, S.A., Hara, H. and Kawamori, A. (1994) Biochim. Biophys. Acta 1186, 91–99.
[20] Astashkin, A.V., Kodera, Y. and Kawamori, A. (1994) Biochim. Biophys. Acta 1187, 89–93.
[21] Kodera, Y., Hara, H., Astashkin, A.V., Kawamori, A. and Ono, T. (1995) Biochim. Biophys. Acta 1232, 43–51.
[22] Milov,A.D., Salikhov,K.M. and Shirov,M.D. (1981) Fiz. Tverd. Tela 23, 975–982.
[23] Milov, A.D., Ponomarev, A.B. and Tsvetkov, Yu.D. (1984) Chem. Phys. Lett. 110, 67–72.
[24] Berthold, D.A., Babcock, G.T. and Yocum, C.F. (1981) FEBS Lett. 134, 231–234.
[25] Ono, T. and Inoue, Y. (1989) Biochim. Biophys. Acta 973, 443–449.
[26] Ono, T. and Inoue, Y. (1988) FEBS Lett. 227, 147–152.
[27] Ono, T. and Inoue, Y. (1992) Biochemistry 31, 7648–7655.